Key Engineering Materials
ISSN: 1662-9795, Vol. 778, pp 189-194
doi:10.4028/www.scientific.net/KEM.778.189

Submitted: 2018-01-06
Revised: 2018-03-01
Accepted: 2018-04-04
Online: 2018-09-05

Structural and Thermoelectric Properties of Gd Doped Bi_2Te_3

FAIZA Arif[a], OMER Farooq[b], FATIMA-Tuz-Zahra[c] and MUHAMMAD Anis-Ur-Rehman[d*]

Applied Thermal Physics Laboratory, Department of Physics, COMSATS Institute of Information Technology, 44000, Islamabad, Pakistan

[a]farif8065@gmail.com, [b]omerfarooq.ciit@gmail.com, [c]fatima.zahra@comsats.edu.pk, [d*]marehman@comsats.edu.pk

Keywords: Thermoelectric Materials, Bismuth Telluride, Electrical Conductivity, Thermal Conductivity, Seebeck Coefficient.

Abstract. The world is currently facing numerous challenges related to energy supply and consumption. Renewable energy sources are very important in view to enhance the worldwide energy needs and environmental effects. One of the important, cost effective and pollution free techniques for renewable energy source is the thermoelectric technology. Thermoelectric materials are of great importance as they convert the heat energy into electrical energy. Thermoelectric materials include tellurides, cobaltites and oxides. In present work, bismuth telluride doped with rare earth metal Gadolinium of different compositions i.e. 0.0 and 0.1 was synthesized by using the simplified sol-gel technique. For structural analysis including crystal structure, phase purity, crystallite size of samples and the lattice parameters, X-ray diffraction (XRD) was used. The structural analysis showed the rhombohedral structure of Bi_2Te_3. AC electrical properties i.e. ac conductivity, loss factor, dielectric constant and impedance studied as a function of frequency (20Hz-3MHz). AC conductivity increased with the increase in frequency while the loss factor, dielectric constant and impedance decreased with the increase in frequency. DC resistivity was analyzed using two probe method at room temperature. Thermal transport properties i.e. thermal conductivity (λ), thermal diffusivity (κ) and volumetric heat capacity(ρCp) are also measured along with the Seebeck coefficient at room temperature.

Introduction

Now-a-days, energy is an important factor. Renewable energy sources play a vital role to enhance the worldwide energy needs [1]. According to a report of International Energy Agency, renewable energy resources share 20% of the world total electricity generation, which will surely increase up to 39% by 2050. It will also purify the atmosphere and remove the presence of carbon dioxide up to 50% [2]. There are many sources of renewable energy like hydro energy, solar energy, wind energy and nuclear energy etc. Thermoelectric materials have applications in solid-state cooling and electric power generation [3]. Thermoelectric materials convert waste heat into electrical energy [4]. The performance of thermoelectric materials depends on different factors, like electrical conductivity (σ), thermal conductivity (κ) and Seebeck coefficient (S). Thermoelectric figure of merit (ZT) is given by the equations $ZT=S^2\sigma T/\lambda$, where S is the Seebeck coefficient, σ is the electrical conductivity, T is temperature and λ is the thermal conductivity [5]. A good thermoelectric material should have a high electrical conductivity and a low thermal conductivity. Bismuth telluride (Bi_2Te_3) is one of the good thermoelectric materials. Bismuth telluride has crystalline structure and is highly anisotropic in nature [6]. Its crystals are made up of hexagonal layers having similar atoms. N-type and p-type materials are used in thermoelectric materials. The band gap of Bi_2Te_3 is 0.2eV, where the thermal conductivity is 3W/mK. The melting point of Bi_2Te_3 is 585^{o}C. Very small amount of rare earth element can enhance the structural properties of the samples. There are many applications of rare earth elements in the field of glass, ceramics, electronics, magnetic, green energy, chemical, catalysts and medical equipment etc. A few elements like Ce and Sm have been studied by different researchers [7].

In this study, the effect of doping is investigated. A small amount of rare earth element i.e., Gadolinium (Gd) is doped in Bi_2Te_3. The crystal structure of Gd is hexagonal. The thermal conductivity of Gd is 0.106 W/cmK. In this work, Bi_2Te_3 doped with rare earth element i.e., Gd of different compositions i.e. 0.0, 0.1 is synthesized by using the simplified sol-gel method. The simplified sol-gel is techniques used for the synthesis of nanoparticles. Sol-gel technique is the best option for the synthesis in this work, because of its high purity [8].

Experimental Methods

Gadolinium doped bismuth telluride with nominal composition $Bi_{2-x}Gd_xTe_3$ (x=0.0, 0.1) was prepared by simplified sol-gel method. To prepare the said composition, bismuth nitrate pentahydrate ($Bi(NO_3)_3.5H_2O$), Gadolinium nitrate hexahydrate ($Gd(NO_3)_3.6H_2O$) and Tellurium (Te), precursors were used in their stoichiometric amounts. Ethylene glycol (EG) was also used in this method as a gelling agent and EG to precursors' mass ratio was optimized at 14:1. Initially, precursors were added into EG in the mentioned ratio and solution was stirred using magnetic hotplate for 30 minutes at room temperature to attain homogeneity. Later, the temperature of the solution was raised up to 80°C and it was stirred at this temperature for 45 minutes. The temperature was then raised up to 120°C for gelatin process. After the gel was formed, to get it burned, temperature was finally increased up to 200°C. The gel was burned at this temperature and powdered sample was attained. Powdered sample was pelletized and sintered at 200°C in vacuum for 5 hours.
The prepared samples were characterized for their structural, electrical, thermal and thermoelectric properties.

Results and Discussion

In this work, structural analysis of the samples $Bi_{2-x}Gd_xTe_3$ (x=0.0 and 0.1) prepared by simplified solgel method was discussed by using X-ray diffraction technique. Electrical analysis such as ac and dc conductivity was done by using two and four probe methods respectively. Seebeck measurements and thermal analysis were also done.
Structural Analysis. The XRD pattern of as-prepared and sintered $Bi_{2-x}Gd_xTe_3$ (x= 0.0 and 0.1) are shown in the Fig. 1(a) and (b).

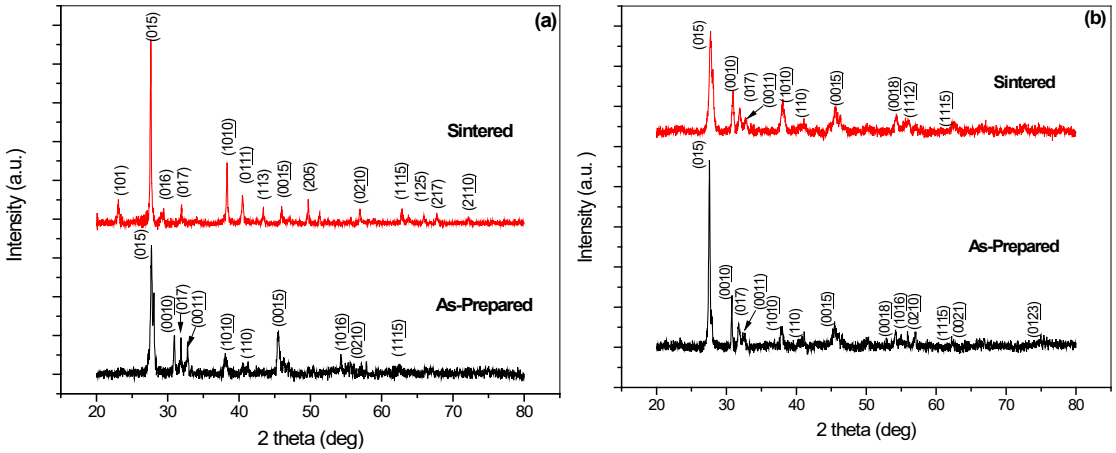

Fig. 1. XRD pattern of as-prepared and sintered samples with compositions (a) x=0.0 and (b) x=0.1

In this work, the structural analysis was done by XRD using a CuK_α source for XRD radiations. All samples are scanned from 20^o to 80^o. The graphs show that both samples were phase pure. Minor change in peaks of sintered samples was due to removal of grain boundary defects after sintering. Both samples had a Rhombohedral structure (space group= R3M). The maximum intensity peak of both samples was present around 27^o and having hkl= (015). The lattice constants calculated for as-prepared and sintered Bi_2Te_3 and $Bi_{1.9}Gd_{0.1}Te_3$ are a=b= 4.38(1) Å, c= 30.465(4) Å.

DC Electrical Analysis. The electrical analysis as a function of temperature of Bi_2Te_3 at room temperature is calculated. By controlling the number and movement of charge carriers, the electrical conductivity can be increased. The charge per carrier is linked to the composition of the samples whereas the carrier mobility is linked to the grain size, defects and boundaries. Nanomaterials have local defects and small conduction barriers, which also increases the conductivity [9]. The DC conductivity of sample with x=0.0 at room temperature is 0.13659 S/cm.

AC Electrical Analysis. In AC electrical analysis, dielectric constant (έ), dielectric loss (tan δ), ac conductivity (σ_{ac}) and impedance (Z) (real and imaginary part) as a function of frequency are measured in the frequency range of 20 Hz to 3 MHz at room temperature. The stacked graphs of $Bi_{2-x}Gd_xTe_3$ (0.0 and 0.1), Bi_2Te_3 and $Bi_{1.9}Gd_{0.1}Te_3$ are shown in the Fig. 2 (a, b, c, d, e, and f).

Dielectric Constant. Dielectric constant (έ) as a function of frequency is calculated by the following equation:

$$\acute{\varepsilon} = Ct/ \varepsilon_o A \quad (1)$$

Where C is the capacitance, ε_o is the relative permittivity of free space and t and A is the thickness and area of the sintered pellet respectively.

Dielectric constant also decreases as the frequency increases. Polarization phenomena greatly affected the response of dielectric constant with changing frequency. Different polarization mechanisms die out at various stages by increasing frequency, because dipoles align themselves.

Dielectric Loss. Dielectric loss factor (**έ**) is the wasted energy and this energy cannot be utilized by the system further. Dielectric loss decreases as the frequency increases. This happens because at the lower frequencies, all type of polarizations present and electrons can easily align themselves, but at higher frequency region, electrons cannot align themselves and hence polarization decreases which results decrease in έ.

AC Conductivity. AC conductivity (σ_{ac}) as a function of frequency was calculated by the following equation:

$$\sigma_{ac} = \omega \varepsilon_o \acute{\varepsilon} \tan\delta \quad (2)$$

Where ω is the angular frequency, ε_o is the relative permittivity of free space (ε_o=8.85x10-^{12}F/m), έ is the dielectric constant and tanδ is the dielectric loss factor. Jump relaxation model is the best way to explain the hopping part of conductivity. This model explains the hopping motion of individual ions [10]. The graph shows that at lower frequency, conductivity is constant then at higher frequency the conductivity increases. This is due to the hopping of electrons start at lower frequencies. Initially, hopping is almost equal (successful and unsuccessful), due to which small variation in conductivity occurs. At higher frequency, the number of successful hopping increases and hence conductivity increases.

Impedance. Impedance as a function of frequency at room temperature was measured in the frequency range of 20 Hz to 3 MHz by using LCR meter. The graphs show that initially the impedance decreased at lower frequency region and then increased at higher frequency region in (x=0.0) case. At lower frequency, less hopping exists, because the polarization is dominant in this region. This happens due to the influence of grain boundaries. The contribution of grain boundaries decreases as the frequency increases and hence impedance decreases. As the space charge polarization depends on frequency, so successful hopping increases at higher frequency region and hence impedance increases. In case of (x=0.1), there exists a constant magnitude of Z at lower frequency and then it decreased at higher frequency.

Impedance (Real Part). Real part of impedance is calculated by the following equation:

$$Z' = Z\cos\theta \quad (3)$$

Real part has the same trend as that of Z. i.e. In case of (x=0.0), Z′decreases at lower frequency range and increases at higher frequency range, while in case of (x=0.1), initially real part has constant magnitude, then decreases at higher frequency.

Impedance (Imaginary Part). Imaginary part of impedance is calculated by the following equation:

$$Z'' = Z \sin\theta \quad (4)$$

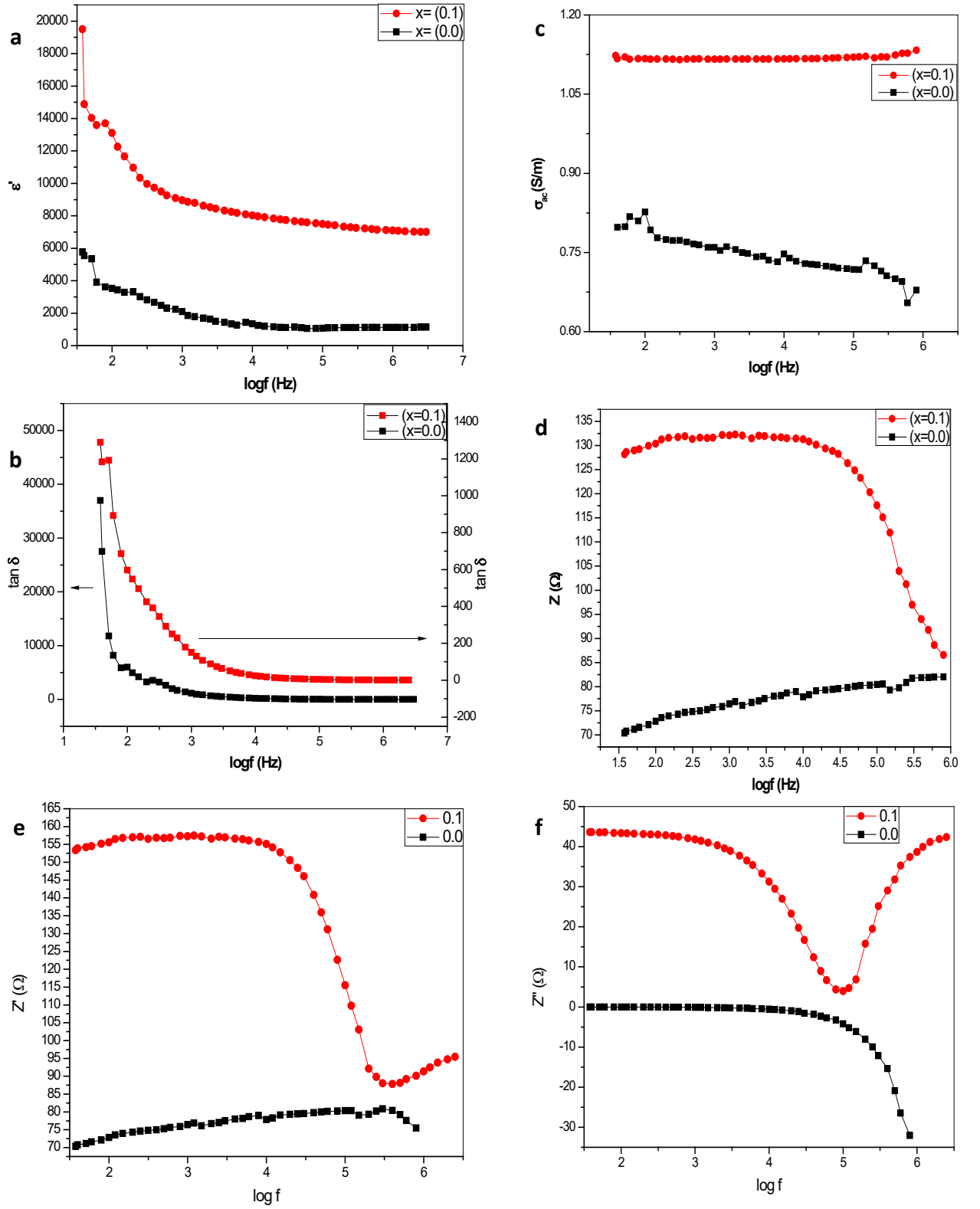

Fig. 2. (a) Plot of έ vs log f of $Bi_{2-x}Gd_xTe_3$ (x=0.0 and 0.1), (b): Plot of tanδ vs log f of $Bi_{2-x}Gd_xTe_3$ (x=0.0 and 0.1), (c) Plot of σ_{ac} vs. log f of $Bi_{2-x}Gd_xTe_3$ (x=0.0 and 0.1), (d). Plot of Z vs. log f of $Bi_{2-x}Gd_xTe_3$ (x=0.0 and 0.1), (e) Plot of Z' vs log f of $Bi_{2-x}Gd_xTe_3$ (x=0.0 and 0.1) (f): Plot of Z'' vs log f of $Bi_{2-x}Gd_xTe_3$ (x=0.0 and 0.1)

The graph shows that Z″ first decreases and then increases. The dip or relaxation peak appears which shifts towards the higher frequency region. This happens due to the increase of loss in the material.

Thermal Transport Measurements. By using advantageous transient plane source method (ATPS), the thermal transport properties i.e. thermal conductivity, thermal diffusivity and specific heat capacity of Bi_2Te_3 and $Bi_{1.9}Gd_{0.1}Te_3$ were measured as a function of temperature**.** Thermal conductivity, thermal diffusivity, volumetric heat capacity and Seebeck co-efficient of the compositions (x=0.0 and 0.1) are shown in the table 1.

The increase in thermal conductivity is due to the growth of crystal that leads to the less scattering of electron and phonon by grain boundaries, [11] while the decrease in thermal conductivity is due to increase in porosity [12]. The results show that thermal conductivity and volumetric heat capacity increased by the addition of dopant while the thermal diffusivity decreased.

The Seebeck co-efficient of sample with x=0.0, at room temperature is calculated. The value of Seebeck co-efficient is -109.4838μV/K. Seebeck co-efficient is negative which shows that the sample exhibits n-type conduction. When both n and p type carriers are present then bipolar effect can take place [13]. The figure of merit value of the same sample is 0.00646 at room temperature, i.e. 303K.

Table 1. Thermal Transport Properties of Bi_2Te_3 and $Bi_{1.9}Gd_{0.1}Te_3$

Compositions	**Thermal Conductivity λ ($Wm^{-1}K^{-1}$)**	**Thermal Diffusivity κ (mm^2s^{-1})**	**Volumetric Heat Capacity ρC_p ($MJm^{-3}K^{-1}$)**
Bi_2Te_3	0.7532	1.07256	0.7011
$Bi_{1.9}Gd_{0.1}Te_3$	0.7838	0.48155	1.6585

Conclusions

$Bi_{2-x}Gd_xTe_3$, (x=0.0 and 0.1) were successfully synthesized by using the simplified sol-gel method. The structural analysis showed that both compositions have rhombohedral structure. DC conductivity of Bi_2Te_3 is also analyzed, having the value of 0.13659 S/cm. AC electrical properties i.e. Dielectric loss tangent (tan δ), dielectric constant (έ), AC conductivity (σ_{ac}), impedance (Z), real part of impedance (Z′) and imaginary part of impedance (Z″) as a function of frequency is also measured, tanδ and έ decreases with the increase in frequency, while the σ_{ac} remains constant at lower frequency and then increased at higher frequency. Z and Z′ also increases as the frequency increases while Z″ decreases initially and then dip appears which shifts towards the higher frequency region. Thermal transport properties (λ, κ and ρCp) of Bi_2Te_3 and $Bi_{1.9}Gd_{0.1}Te_3$ showed that thermal conductivity and volumetric heat capacity increases and thermal diffusivity decreased by the addition of dopant. Seebeck co-efficient having the value -109.48μV/K, shows that sample exhibits n-type conduction. Studied materials could be used in thermoelectric applications for power generation.

Acknowledgement

Higher Education Commission (HEC) of Pakistan is acknowledged for providing the financial support through NRPUNo. 3429, for this research.

References

[1] J. Goldemberg, Energy and challenge of sustainability, World Energy Assessment: United Nations Publications. (2000).

[2] M. Bhattacharya, S.R. Paramati, I. Ozturk, S. Bhattacharya, The effect of renewable energy consumption on economic growth: Evidence from top 38 countries, App. Ener., 162 (2016) 733-741.

[3] X.B. Zhao, X.H. Ji, Y.H. Zhang, T.J. Zhu, J.P. Tu, X.B. Zhang, Bismuth telluride nanotubes and the effects on the thermoelectric properties of nanotubes-containing nanocomposites, Appl. Phys. Lett., 86 (2005) 062111.

[4] T.M. Tritt, M.A. Subramanian, Thermoelectric materials, phenomena, and applications: A bird's eye view, Guest Editors. 31 (2006) 188-198.

[5] T.C. Harman, M.P. Walsh, B.E. Laforge, G.W. Turner, Nanostructured thermoelectric materials, J. Electron. Mater., 34 (2005) 19-22.

[6] B.S. Kin, J.H. Yang, H.S. Dow, M.W. Oh, S.D. Park, H.W. Lee, D.S. Bae, Thermoelectric properties of Bi_2Te_3 material doped with lanthanum by mechanical alloying, Taylor and Francis. 38 (2008) 143-147.

[7] Q. Lin, J. Lin, Y. He, R. Wang, J. Dong, The structural and magnetic properties of gadolinium doped $CoFe_2O_4$ nanoferrites, J. Nanomat., 8 (2015) 82-87.

[8] S. Nasir, M. Anis-ur-Rehman, Structural, electrical and magnetic studies of nickel-zinc nanoferrites prepared by simplified solgel and co-precipitation methods, Phys. Scr., 84 (2011) 025603.

[9] J. Zhou, C. Jim, J. H. Seol, X. Li, L. Shi, Thermoelectric properties of individual electrodeposited bismuth telluride nanowires, Appl. Phys. Lett., 87 (2005) 133109.

[10] K. Funke, Jump relaxation model and coupling model- a comparison, J. Non Crys. Solids., 172-174 (1994) 1215-1221.

[11] M. Yaprintsev, R. Lyubushkin, O. Soklakova, O. Ivanov, Microstructure and thermoelectric properties of $Bi_{1.9}Lu_{0.1}Te_3$ compound, Rare Metals., 12 (2017) 1-8.

[12] M. Takashiri, S. Tanaka, H. Hagino, K. Miyazaki, Combined effect of nanoscale grain size and porosity on lattice thermal conductivity of bismuth-telluride-based bulk alloys, J. Appl Phys., 112 (2012) 084315.

[13] F. Wu, W. Wang, X. Hu, M. Tang, Thermoelectric properties of I-doped n-type Bi_2Te_3-based material prepared by hydrothermal and subsequent hot pressing, Prog. Nat. Sci.: Mater. Internat., 27 (2017) 203-207.